coatings

MDPI

Supplementary Materials: Effect of Carrier Gas on the Gas Sensing Performance of $Co_{1-2x}Ni_xMn_xFe_{2-y}Ce_yO_4$ Double-Substitution Spinel in Flammable Gases and Volatile Organic Compounds

Sunday A. Ogundipe [1,*], Ceboliyazakha L. Ndlangamandla [1], Mmantsae M. Diale [2], Mudalo Jozela [3], Hendrik C. Swart [4], David E. Motaung [4] and Steven S. Nkosi [5,*]

[1] Department of Physics, University of Zululand, Private Bag X1001, KwaDlangezwa 3886, South Africa; ndlangamandlac@unizulu.ac.za
[2] Department of Physics, University of Pretoria, Private Bag X20, Hatfield 0028, South Africa; mmantsae.diale@up.ac.za
[3] National Metrology Institute of South Africa (NMISA), CSIR Campus, Building 5, Meiring Naude Road, Brummeria, Pretoria 0182, South Africa; mjozela@nmisa.co.za
[4] Department of Physics, University of the Free State, P.O. Box 339, Bloemfontein 9300, South Africa; swarthc@ufs.ac.za (H.C.S.); david.e.motaung@gmail.com (D.E.M.)
[5] Department of Physics, University of Limpopo, Private Bag X1106, Sovenga 0727, South Africa
* Correspondence: ogundipesunday6@gmail.com (S.A.O.); steven.solethu.nkosi@gmail.com (S.S.N.)

Citation: Ogundipe, S.A.; Ndlangamandla, C.L.; Diale, M.M.; Jozela, M.; Swart, H.C.; Motaung, D.E.; Nkosi, S.S. Effect of Carrier Gas on the Gas Sensing Performance of $Co_{1-2x}Ni_xMn_xFe_{2-y}Ce_yO_4$ Double-Substitution Spinel in Flammable Gases and Volatile Organic Compounds. *Coatings* **2023**, *13*, x. https://doi.org/10.3390/xxxxx

Academic Editor: M. Shaheer Akhtar

Received: 30 August 2023
Revised: 5 October 2023
Accepted: 11 October 2023
Published: date

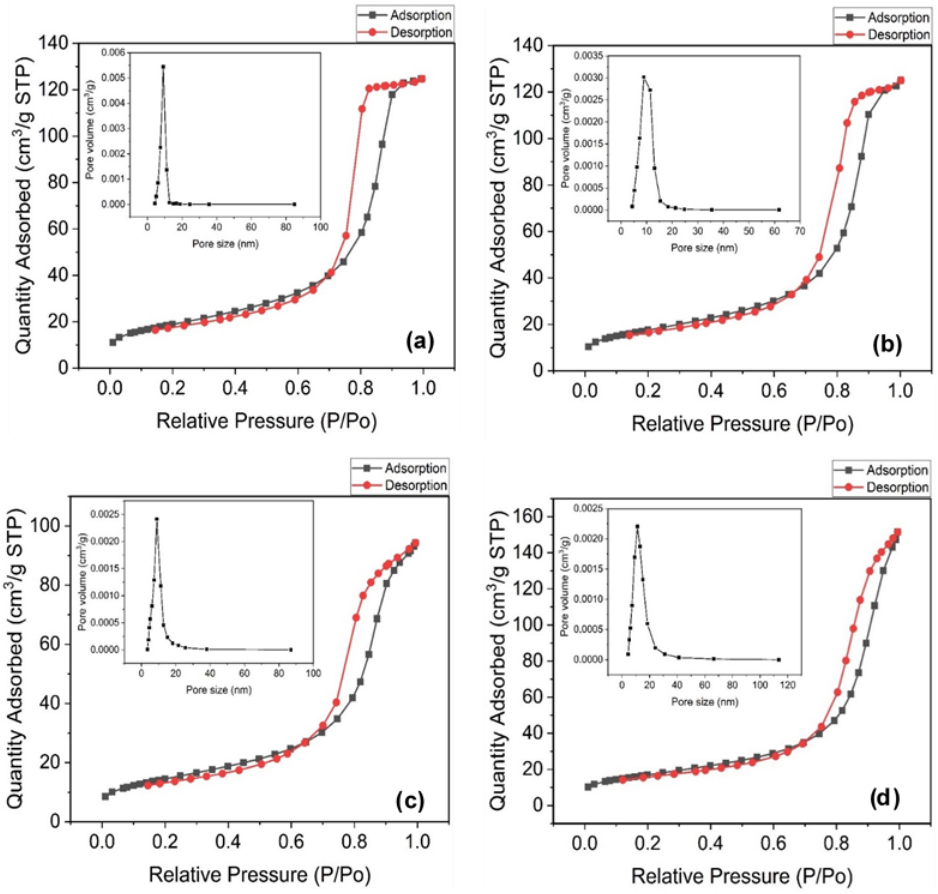

Figure S1. Nitrogen adsorption-desorption isotherms of $Co_{1-2x}Ni_xMn_xFe_{2-y}Ce_yO_4$ samples with (a) x = y = 0: dried with infrared lamp, (b) x = y = 0: dried naturally, (c) x = y = 0.2 and (d) x = y = 0.3. **Insets**: The corresponding pore size distribution.

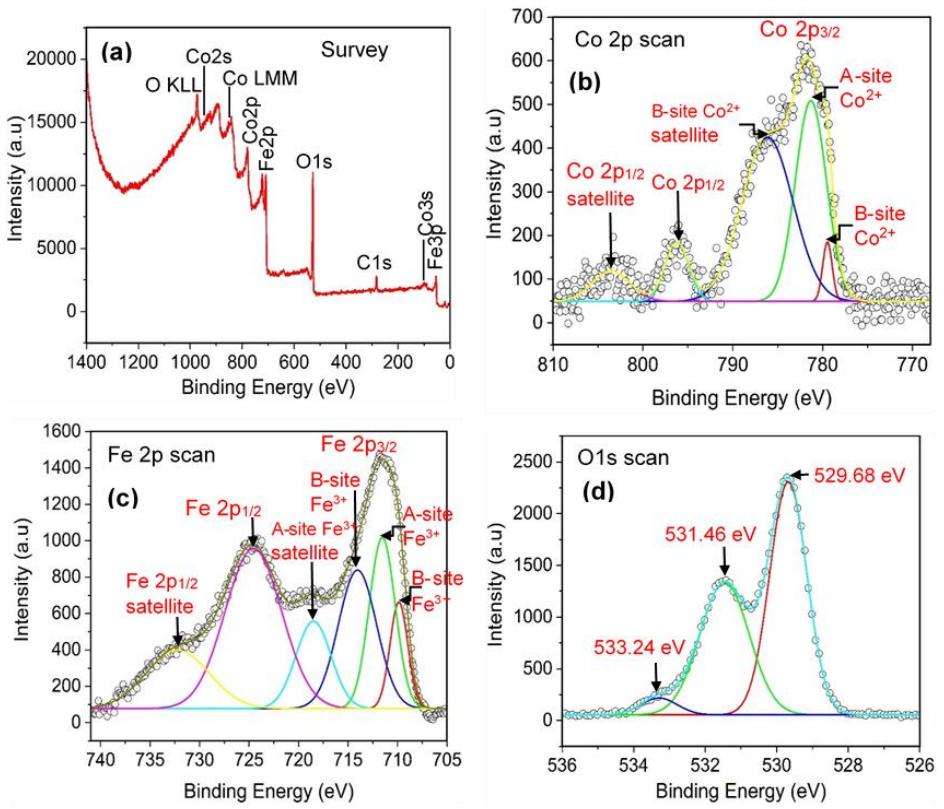

Figure S2. (a) Survey spectrum, before sputtering, of $CoFe_2O_4$ samples. XPS spectra of $Co_{1-2x}Ni_xMn_xFe_{2-y}Ce_yO_4$ sample for which x = y = 0 (lamp-dried): (b) Co 2p scan, (c) Fe 2p scan, and (d) O 1s scan.

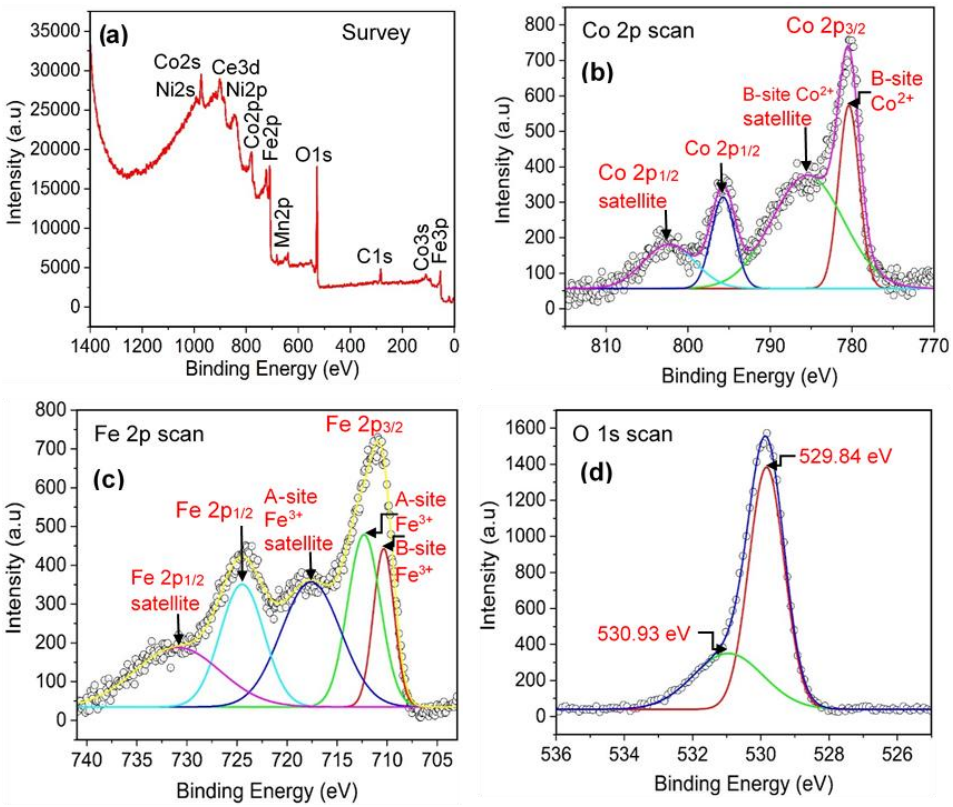

Figure S3. (a) Survey spectrum, before sputtering, of $Co_{1-2x}Ni_xMn_xFe_{2-y}Ce_yO_4$ samples. XPS spectra of $Co_{1-2x}Ni_xMn_xFe_{2-y}Ce_yO_4$ sample for which x = y = 0 (natural-dried): (b) Co 2p scan, (c) Fe 2p scan, and (d) O 1s scan.

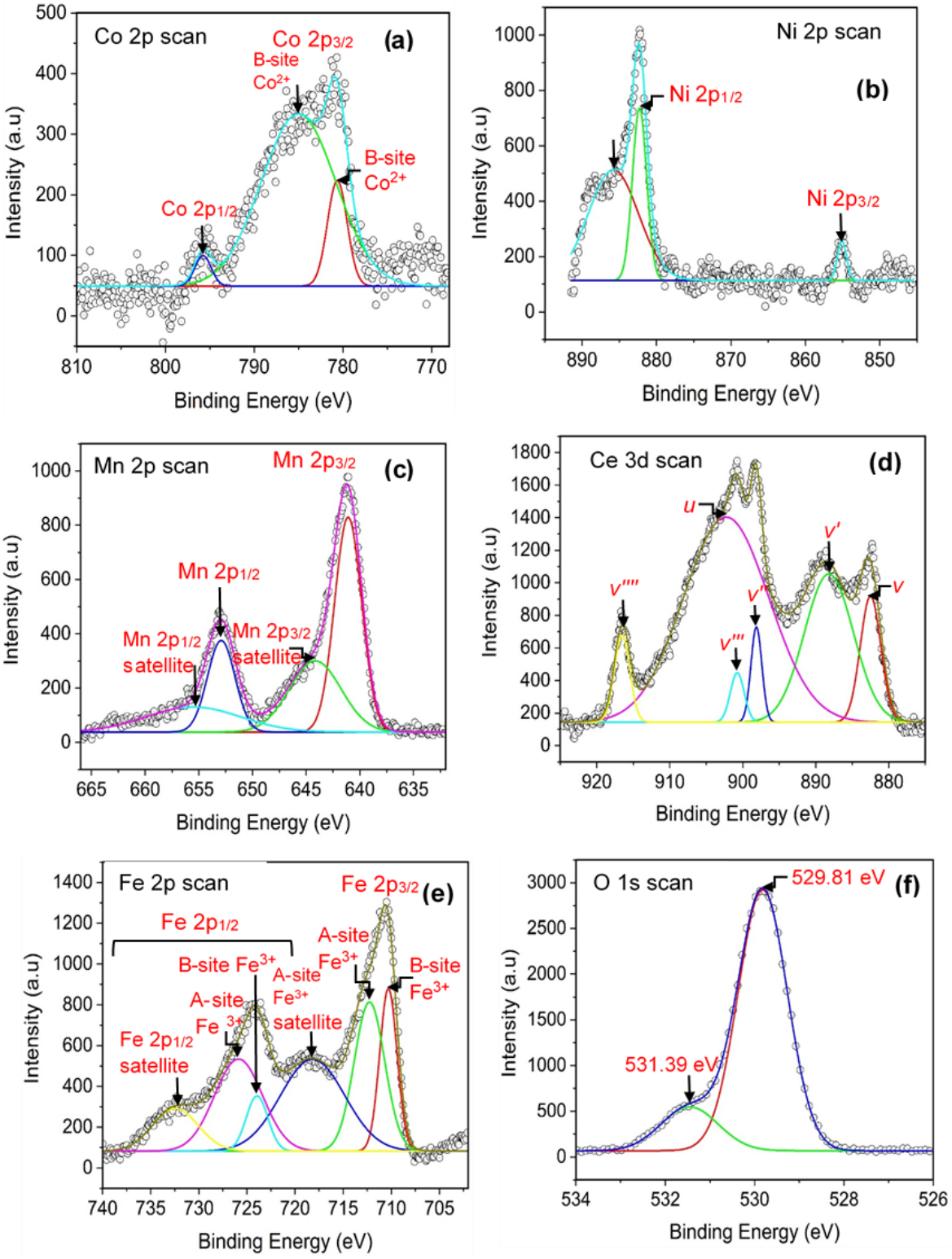

Figure S4. XPS spectra of $Co_{1-2x}Ni_xMn_xFe_{2-y}Ce_yO_4$ sample for which x = y = 0.2: (a) Co 2p scan, (b) Ni 2p scan, (c) Mn 2p scan (d) Ce 3d scan, (e) Fe 2p scan, and (f) O 1s scan.

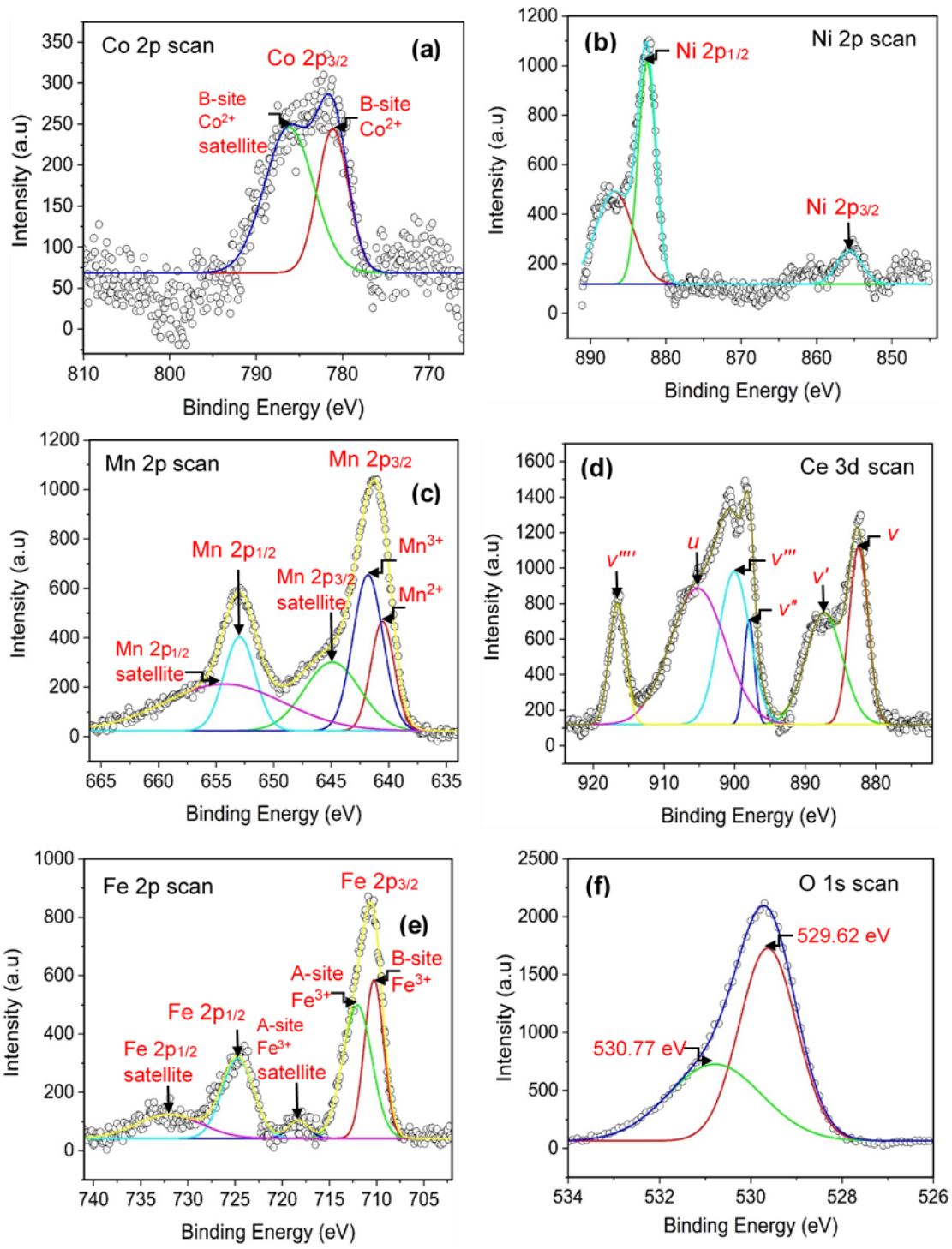

Figure S5. XPS spectra of $Co_{1-2x}Ni_xMn_xFe_{2-y}Ce_yO_4$ sample for which x = y = 0.3: (a) Co 2p scan, (b) Ni 2p scan, (c) Mn 2p scan (d) Ce 3d scan, (e) Fe 2p scan, and (f) O 1s scan.

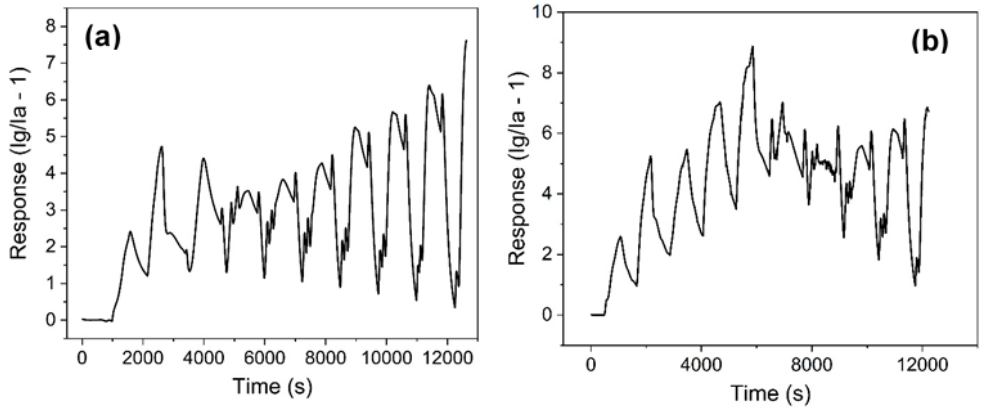

Figure S6. Gas sensing response pattern of: **(a)** S3 towards LPG using nitrogen as carrier gas, **(b)** S2 towards LPG using argon as carrier gas.

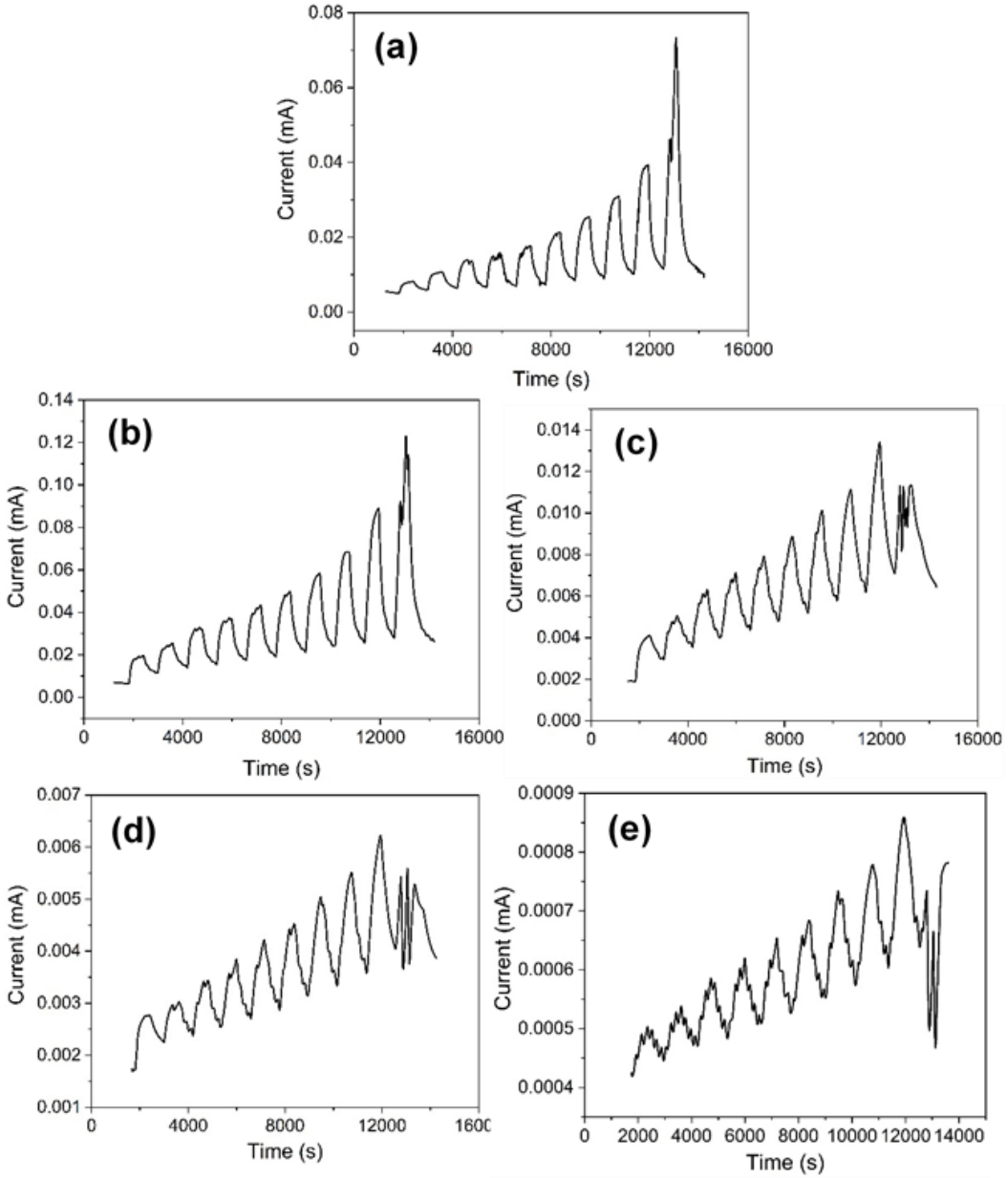

Figure S7. The transient current curve of (a) S1, (b) S2, (c) S3, (d) S4, and (e) S5 towards LPG using dry air as carrier gas at 175 °C.

Table S1. Fitting peaks in Figures S4(d) and S5(d) and the respective cations.

Peak	cation
V	Ce^{4+}
V’	Ce^{4+}
V’’	Ce^{4+}
V’’’	Ce^{4+}
V’’’’	Ce^{4+}
U	$Ce3^{+}$